A

T_{RM} cell absolute numbers

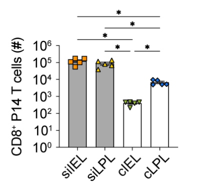

siIEL | siLPL | cIEL | cLPL

B GzmA

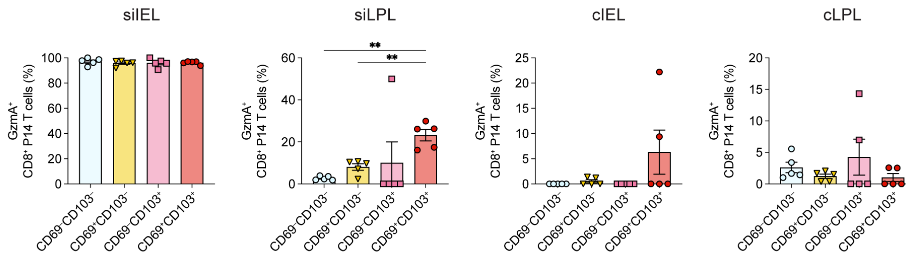

C GzmB

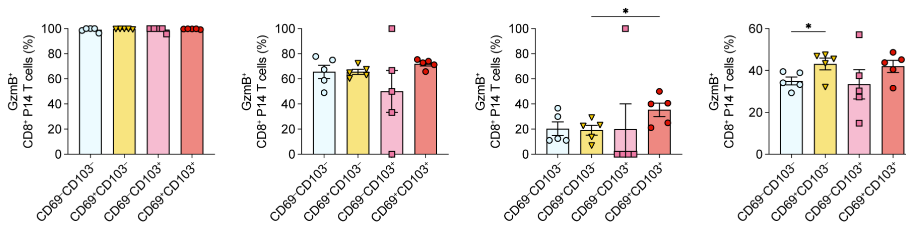

D TNF

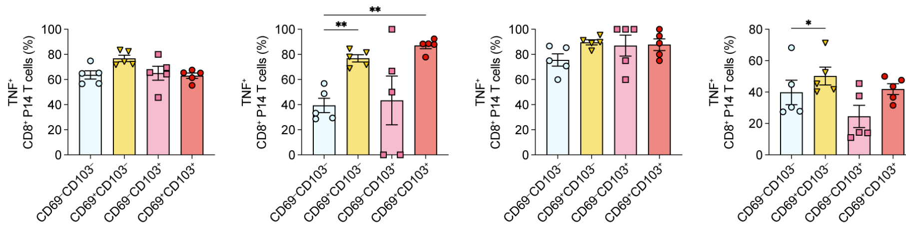

E IFNγ

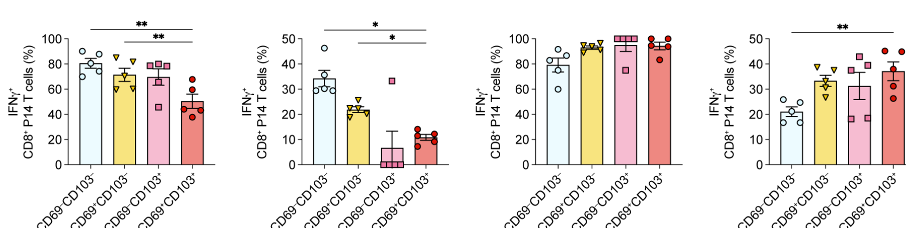

F IL-2

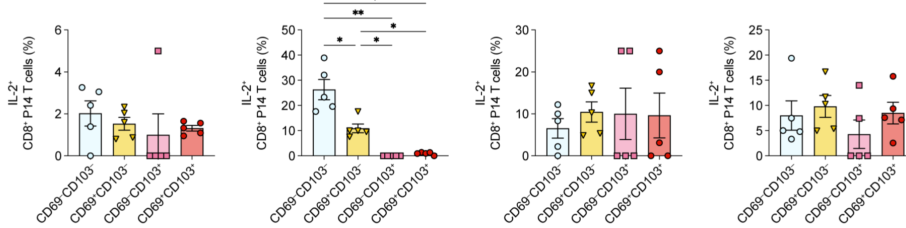

G CD127

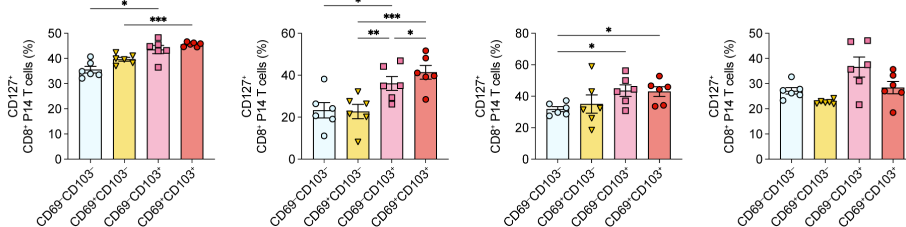

Figure S1. Phenotypic and functional characteristics of $CD69^{-}CD103^{-}$, $CD69^{+}CD103^{-}$, $CD69^{-}CD103^{+}$, and $CD69^{+}CD103^{+}$ intestinal $CD8^{+}$ T_{RM} cells, Related to Figures 1 and 2.

(A) Absolute numbers of gated i.v.-negative $CD45.1^{+}CD8\beta^{+}$ P14 T cells in each intestinal tissue compartment.

(B–G) Bar graphs representing frequencies of $CD69^{-}CD103^{-}$ (light blue circles), $CD69^{+}CD103^{-}$ (yellow inverted triangles), $CD69^{-}CD103^{+}$ (pink squares), or $CD69^{+}CD103^{+}$ (red circles) cells expressing GzmA (**B**), GzmB (**C**), TNF (**D**), IFNγ (**E**), IL-2 (**F**), and CD127 (**G**) in gated i.v.-negative $CD45.1^{+}CD8\beta^{+}$ P14 T cells from the siIEL, siLPL, cIEL, and cLPL intestinal tissue compartments. For analyses of TNF, IFNγ, and IL-2, cells were restimulated *in vitro* for 3h with $gp_{33\text{-}41}$ peptide.

Data are represented as mean ± SEM. Repeated measures one-way ANOVA. *$p<0.05$, **$p<0.01$, ***$p<0.001$ ****$p<0.0001$. Data are representative of at least 3 independent experiments with n=5-6 mice per experiment.

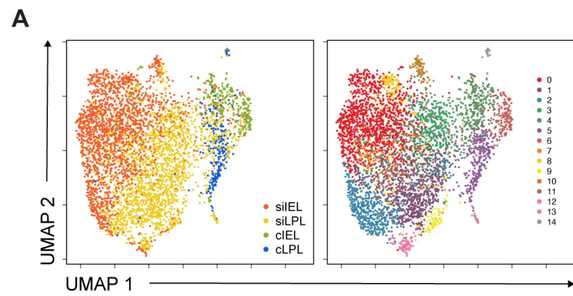
A
UMAP 2
UMAP 1
siIEL
siLPL
cIEL
cLPL
0
1
2
3
4
5
6
7
8
9
10
11
12
13
14

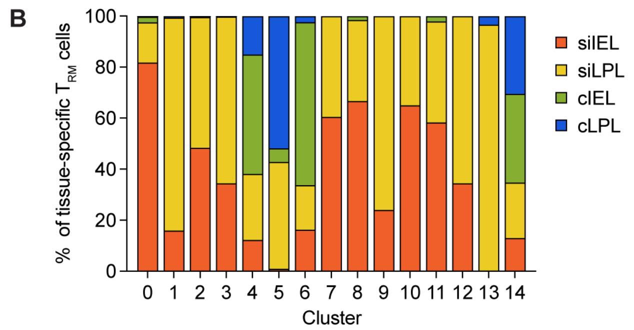
B
% of tissue-specific T_{RM} cells
100
80
60
40
20
0
0 1 2 3 4 5 6 7 8 9 10 11 12 13 14
Cluster
siIEL
siLPL
cIEL
cLPL

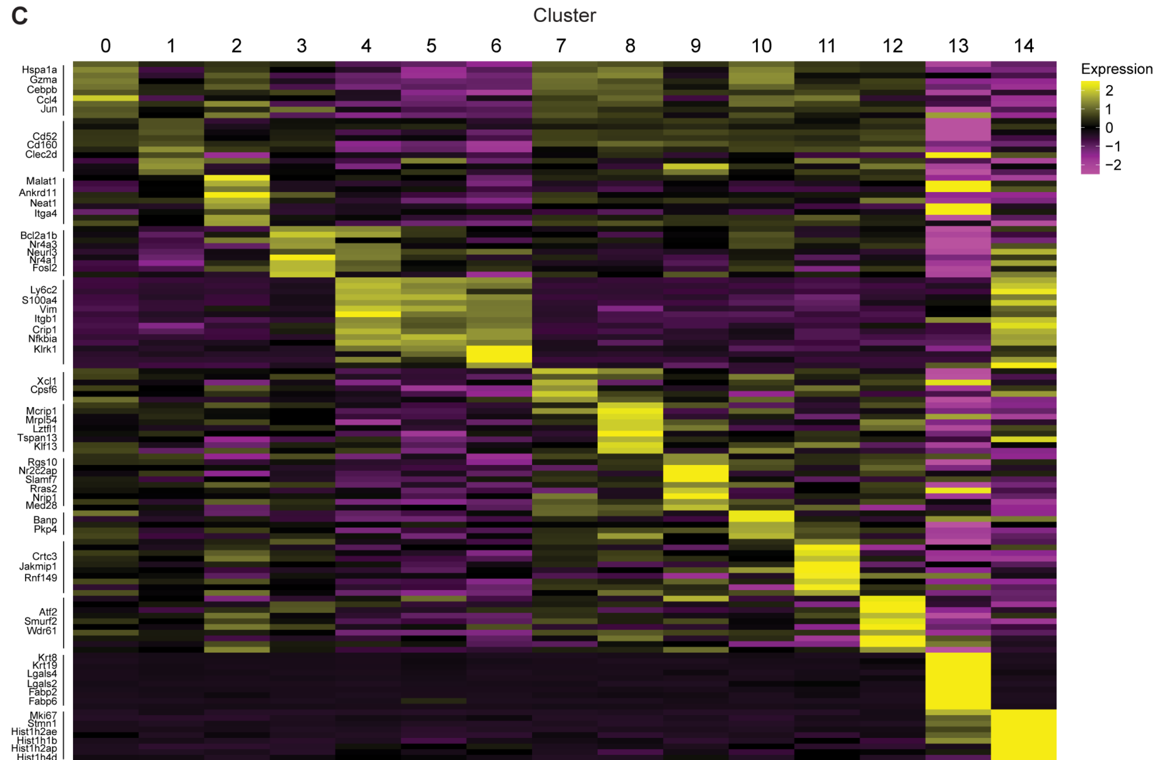
C
Cluster
0 1 2 3 4 5 6 7 8 9 10 11 12 13 14
Expression
2
1
0
−1
−2
Hspa1a
Gzma
Cebpb
Ccl4
Jun
Cd52
Cd160
Clec2d
Malat1
Ankrd11
Neat1
Itga4
Bcl2a1b
Nr4a3
Neurl3
Nr4a1
Fosl2
Ly6c2
S100a4
Vim
Itgb1
Crip1
Nfkbia
Klrk1
Xcl1
Cpsf6
Mcrip1
Mrpl54
Lztfl1
Tspan13
Klf13
Rgs10
Nr2c2ap
Slamf7
Rras2
Nrip1
Med28
Banp
Pkp4
Crtc3
Jakmip1
Rnf149
Atf2
Smurf2
Wdr61
Krt8
Krt19
Lgals4
Lgals2
Fabp2
Fabp6
Mki67
Stmn1
Hist1h2ae
Hist1h1b
Hist1h2ap
Hist1h4d

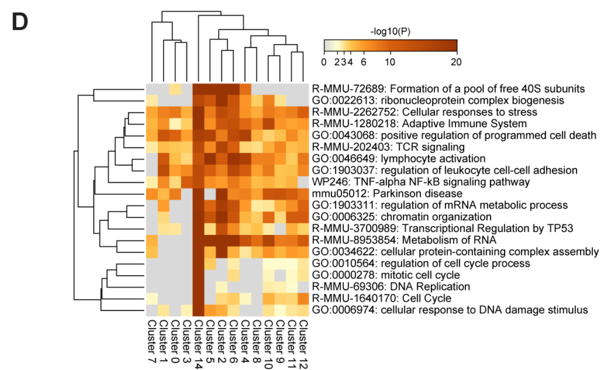
D
-log10(P)
0 2 3 4 6 10 20
R-MMU-72689: Formation of a pool of free 40S subunits
GO:0022613: ribonucleoprotein complex biogenesis
R-MMU-2262752: Cellular responses to stress
R-MMU-1280218: Adaptive Immune System
GO:0043068: positive regulation of programmed cell death
R-MMU-202403: TCR signaling
GO:0046649: lymphocyte activation
GO:1903037: regulation of leukocyte cell-cell adhesion
WP246: TNF-alpha NF-kB signaling pathway
mmu05012: Parkinson disease
GO:1903311: regulation of mRNA metabolic process
GO:0006325: chromatin organization
R-MMU-3700989: Transcriptional Regulation by TP53
R-MMU-8953854: Metabolism of RNA
GO:0034622: cellular protein-containing complex assembly
GO:0010564: regulation of cell cycle process
GO:0000278: mitotic cell cycle
R-MMU-69306: DNA Replication
R-MMU-1640170: Cell Cycle
GO:0006974: cellular response to DNA damage stimulus
Cluster 7
Cluster 1
Cluster 0
Cluster 3
Cluster 14
Cluster 5
Cluster 2
Cluster 6
Cluster 4
Cluster 8
Cluster 10
Cluster 9
Cluster 11
Cluster 12

Figure S2. Transcriptional heterogeneity exhibited by $CD8^+$ T_{RM} cells from small intestine and colon, Related to Figure 3. $CD8^+$ P14 T cells harvested from siIEL, siLPL, cIEL, and cLPL tissue compartments were FACS-purified more than 21 days after LCMV infection and processed for CITE-seq with the 10x Genomics platform.

(A) UMAP clustering of all $CD8\beta^+$ P14 T_{RM} cells from each intestinal tissue compartment, colored by tissue compartment identity (left) or cluster identity (right).

(B) Bar graph representing the composition of each cell cluster based on intestinal tissue compartment.

(C) Top ten genes differentially expressed by each UMAP cluster, represented as a hierarchically clustered summary heatmap; rows represent individual genes and columns represent each UMAP cluster. Selected genes are highlighted on the left.

(D) Comparative gene ontology analyses performed on all UMAP clusters, represented as a summary heatmap.

A

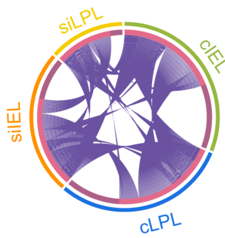

B

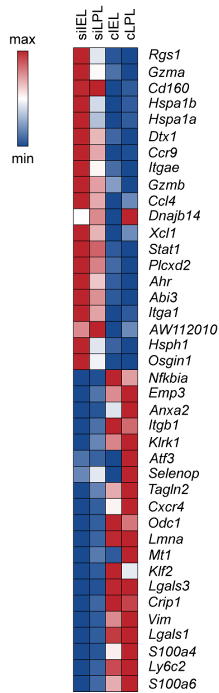

C

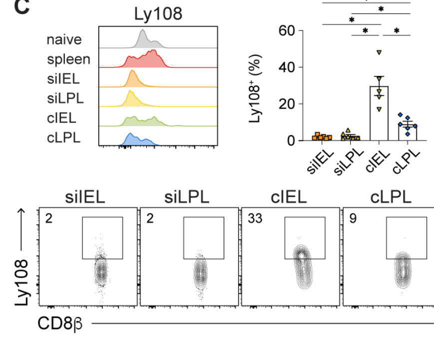

D

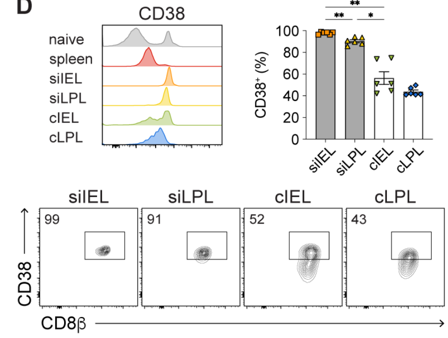

E

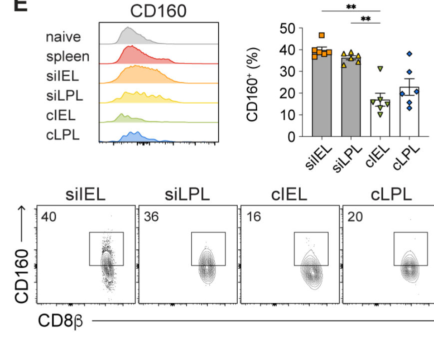

F

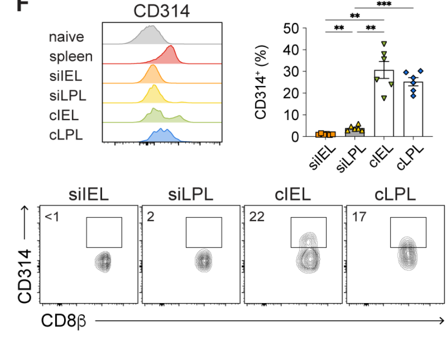

G

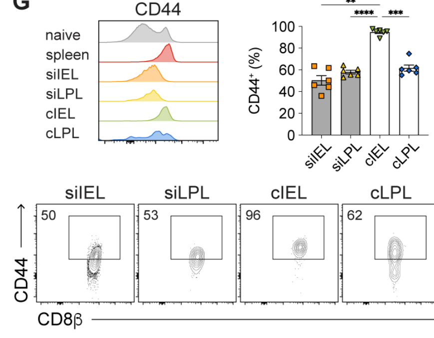

H

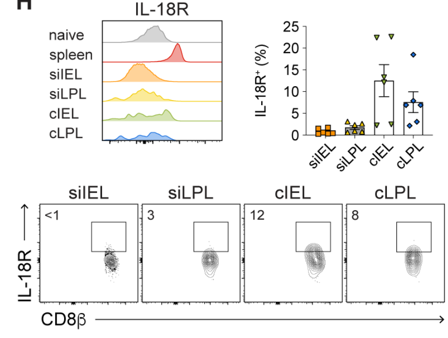

Figure S3. Heterogeneity at the mRNA and protein levels exhibited by $CD8^+$ T_{RM} cells from small intestine and colon, Related to Figure 3.

(A) Differentially expressed genes shared among $CD8\beta^+$ P14 T_{RM} cells from the siIEL, siLPL, cIEL, and cLPL intestinal tissue compartments, represented as a Circos plot. Inner circle represents gene lists, and purple curves link identical (shared) genes; outer circle represents tissue compartment identity.

(B) Top twenty genes differentially expressed between small intestine vs. colon $CD8^+$ T_{RM} cells, represented as a hierarchically clustered summary heatmap; rows represent individual genes and columns represent each of the 4 intestinal tissue compartments.

(C–H) Representative flow cytometry plots (bottom) showing expression of Ly108 (**C**), CD38 (**D**), CD160 (**E**), CD314 (**F**), CD44 (**G**), and IL-18R (**H**) by gated i.v.-negative $CD45.1^+CD8\beta^+$ P14 T cells from the four intestinal tissue compartments; numbers represent the frequencies of cells within each gate. Bar graphs (top right) indicate the frequencies of P14 T cells expressing each molecule. Histograms (top left) indicate the distribution of expression of each marker by P14 T cells from each of the four intestinal tissue compartments and the spleen; expression by naïve ($CD62L^{hi}CD44^{lo}$) $CD8\beta^+$ T cells from a separate uninfected mouse is shown for comparison.

Data are represented as mean ± SEM. Repeated measures one-way ANOVA. *$p<0.05$, **$p<0.01$, ***$p<0.001$ ****$p<0.0001$. Data are representative of at least 3 independent experiments with n=5-6 mice per experiment.

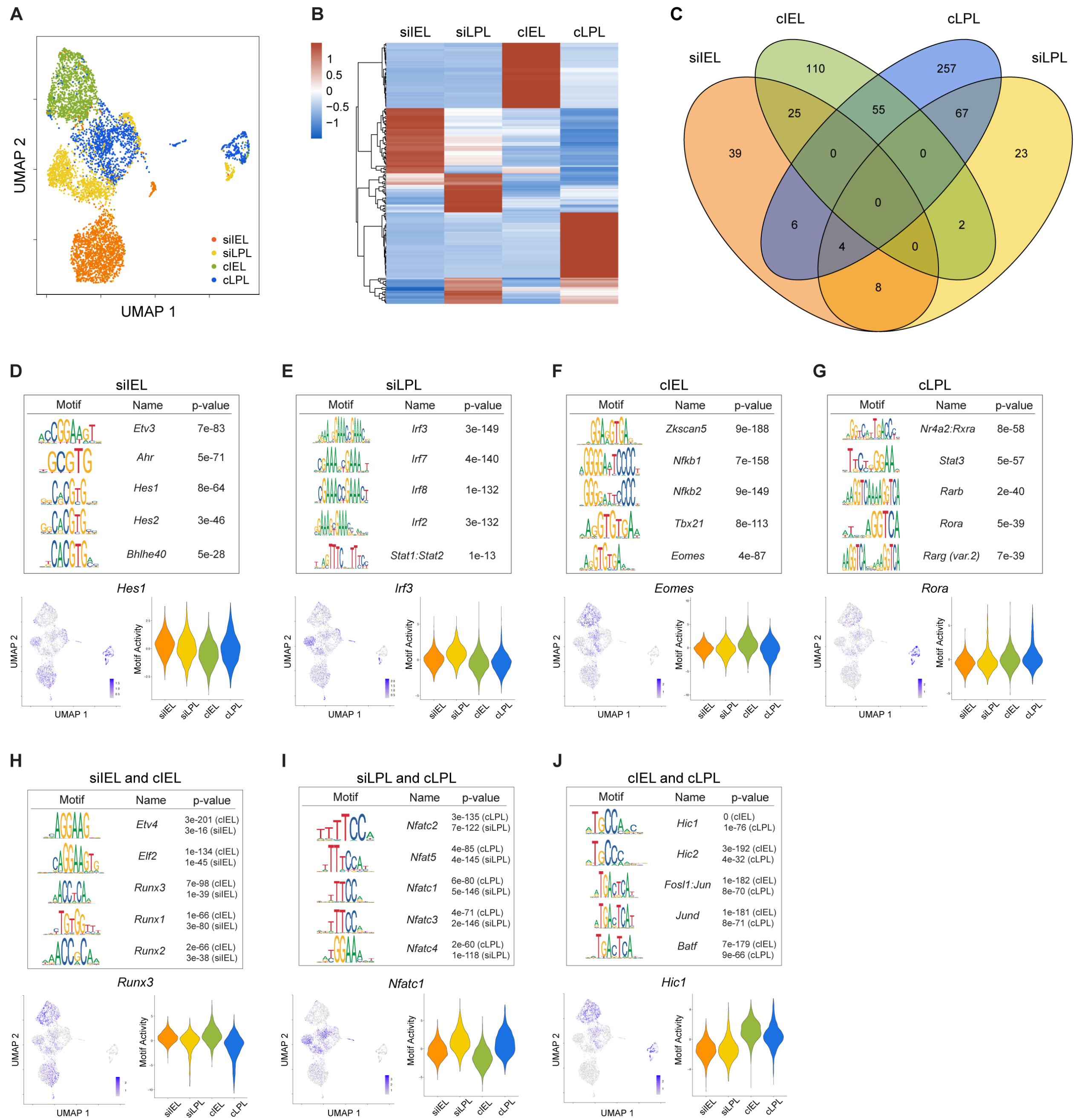
A
UMAP 2
UMAP 1
siIEL
siLPL
cIEL
cLPL
B
siIEL
siLPL
cIEL
cLPL
1
0.5
0
−0.5
−1
C
cIEL
cLPL
siIEL
siLPL
110
257
25
55
67
39
0
0
23
0
6
2
4
0
8
D
siIEL
Motif
Name
p-value
Etv3
7e-83
Ahr
5e-71
Hes1
8e-64
Hes2
3e-46
Bhlhe40
5e-28
Hes1
E
siLPL
Motif
Name
p-value
Irf3
3e-149
Irf7
4e-140
Irf8
1e-132
Irf2
3e-132
Stat1:Stat2
1e-13
Irf3
F
cIEL
Motif
Name
p-value
Zkscan5
9e-188
Nfkb1
7e-158
Nfkb2
9e-149
Tbx21
8e-113
Eomes
4e-87
Eomes
G
cLPL
Motif
Name
p-value
Nr4a2:Rxra
8e-58
Stat3
5e-57
Rarb
2e-40
Rora
5e-39
Rarg (var.2)
7e-39
Rora
Motif Activity
H
siIEL and cIEL
Motif
Name
p-value
Etv4
3e-201 (cIEL)
3e-16 (siIEL)
Elf2
1e-134 (cIEL)
1e-45 (siIEL)
Runx3
7e-98 (cIEL)
1e-39 (siIEL)
Runx1
1e-66 (cIEL)
3e-80 (siIEL)
Runx2
2e-66 (cIEL)
3e-38 (siIEL)
Runx3
I
siLPL and cLPL
Motif
Name
p-value
Nfatc2
3e-135 (cLPL)
7e-122 (siLPL)
Nfat5
4e-85 (cLPL)
4e-145 (siLPL)
Nfatc1
6e-80 (cLPL)
5e-146 (siLPL)
Nfatc3
4e-71 (cLPL)
2e-146 (siLPL)
Nfatc4
2e-60 (cLPL)
1e-118 (siLPL)
Nfatc1
J
cIEL and cLPL
Motif
Name
p-value
Hic1
0 (cIEL)
1e-76 (cLPL)
Hic2
3e-192 (cIEL)
4e-32 (cLPL)
Fosl1:Jun
1e-182 (cIEL)
8e-70 (cLPL)
Jund
1e-181 (cIEL)
8e-71 (cLPL)
Batf
7e-179 (cIEL)
9e-66 (cLPL)
Hic1
UMAP 2
UMAP 1
Motif Activity
siIEL
siLPL
cIEL
cLPL

Figure S4. Epigenetic heterogeneity exhibited by CD8$^+$ T_{RM} cells from small intestine and colon, Related to Figure 3.

(A) UMAP clustering analyses of scATAC-seq data from CD8β$^+$ P14 T_{RM} cells from the siIEL, siLPL, cIEL, and cLPL intestinal tissue compartments.

(B) Top differentially accessible chromatin regions, represented as a hierarchically clustered summary heatmap; rows represent regions and columns represent each of the 4 intestinal tissue compartments.

(C) Venn diagram analysis of preferentially enriched and shared transcription factor motifs identified in accessible chromatin regions from each of the 4 intestinal tissue compartments.

(D–J) Examples of transcription factor motifs (top) preferentially enriched (**D**–**G**) or shared (**H**–**J**) in accessible chromatin regions from each of the 4 intestinal tissue compartments. Motif activity for selected genes is represented as violin plots (middle) or superimposed onto UMAP embeddings (bottom).

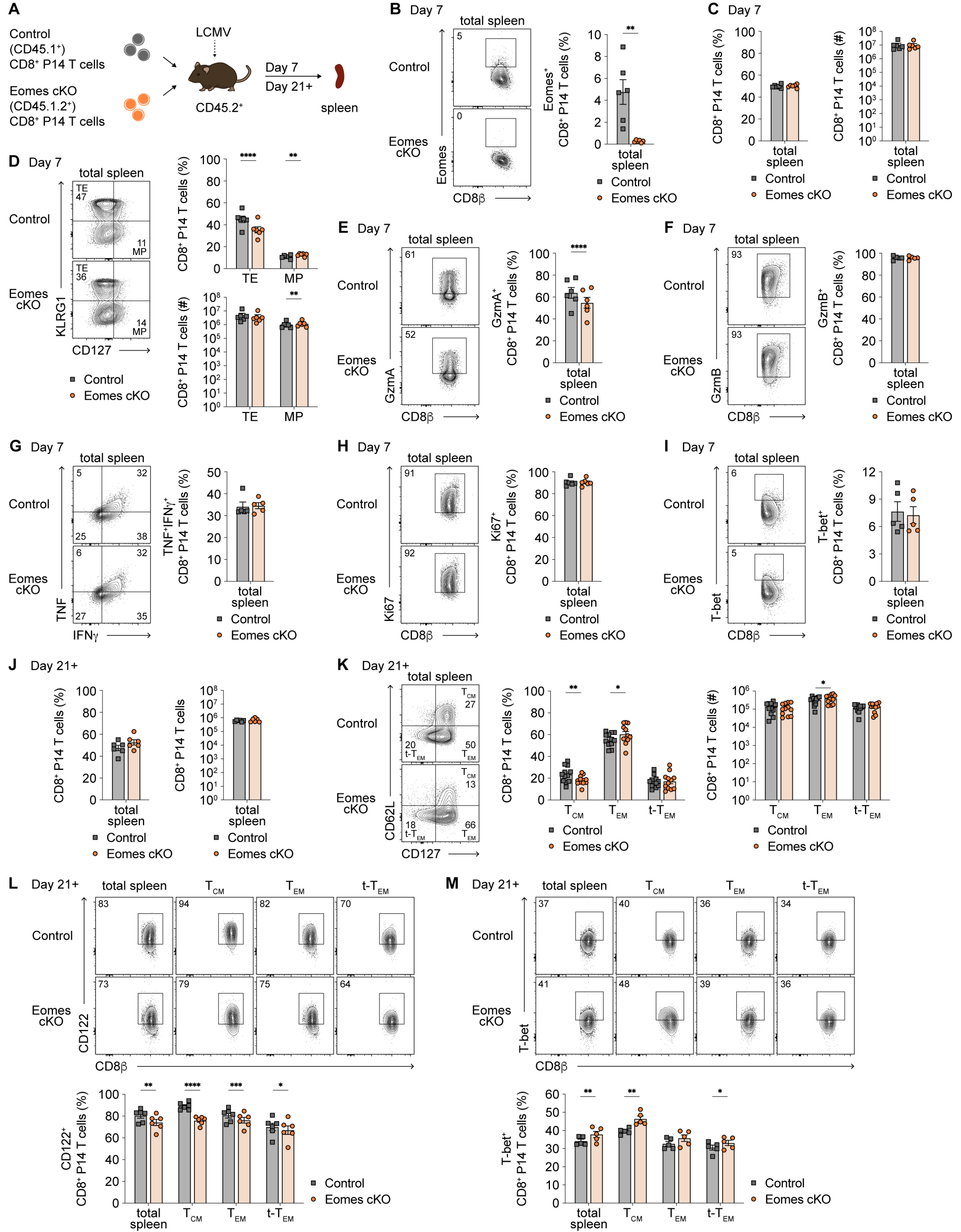

Figure S5. Deficiency of Eomes has modest effects on effector $CD8^+$ T cell differentiation in the spleen, Related to Figure 5.

(A) Experimental design. $CD8^+$ P14 T cells from control ($CD45.1^+$) and *Eomes*$^{fl/fl}$*Cd4-Cre*$^+$($CD45.1.2^+$, Eomes cKO) mice were mixed at a 1:1 ratio and adoptively co-transferred into congenic $CD45.2^+$ recipients prior to infection with LCMV. P14 T cells were isolated from spleen at 7 days (**B–I**) or after 21 days (**J–M**) following infection.

(B and E–I) Representative flow cytometry plots (left) and bar graphs (right) displaying frequencies of control (grey squares) vs. Eomes cKO (orange circles) P14 T cells expressing Eomes (**B**), GzmA (**E**), GzmB (**F**), TNF and IFNγ (**G**), Ki67 (**H**), or T-bet (**I**) at 7 days following infection; numbers represent the frequencies of cells within each gate. For analyses of TNF and IFNγ, cells were restimulated *in vitro* for 3h with gp_{33-41} peptide.

(C and J) Quantification of the proportions (left) or absolute numbers (right) of control vs. Eomes cKO P14 T cells in the spleen at 7 days (**C**) or after 21 days (**J**) following infection.

(D) Representative flow cytometry plots (left) displaying KLRG1 and CD127 expression by control vs. Eomes cKO P14 T cells in the spleen at 7 days following infection. Bar graphs representing proportions (top right) or absolute numbers (bottom right) of control vs. Eomes cKO P14 T cells in the spleen exhibiting a terminal effector ('TE', $KLRG1^{hi}CD127^{lo}$) or memory precursor ('MP', $KLRG1^{lo}CD127^{hi}$) phenotype.

(K) Representative flow cytometry plots (left) and bar graphs indicating the frequencies (middle) and absolute numbers (right) of control vs. Eomes cKO T_{CM} ($CD62L^{hi}CD127^{hi}$), T_{EM} ($CD62L^{lo}CD127^{hi}$), and t-T_{EM} ($CD62L^{lo}CD127^{lo}$) cells after 21 days following infection.

(L and M) Representative flow cytometry plots (top) and bar graphs (bottom) displaying CD122 (**L**) and T-bet (**M**) expression by control vs. Eomes cKO T_{CM} ($CD62L^{hi}CD127^{hi}$), T_{EM} ($CD62L^{lo}CD127^{hi}$), and t-T_{EM} ($CD62L^{lo}CD127^{lo}$) cells after 21 days following infection.

Data are represented as mean ± SEM. Paired *t*-test. *$p<0.05$, **$p<0.01$, ***$p<0.001$ ****$p<0.0001$. Data are representative of at least 3 independent experiments with n=5-6 mice per experiment.

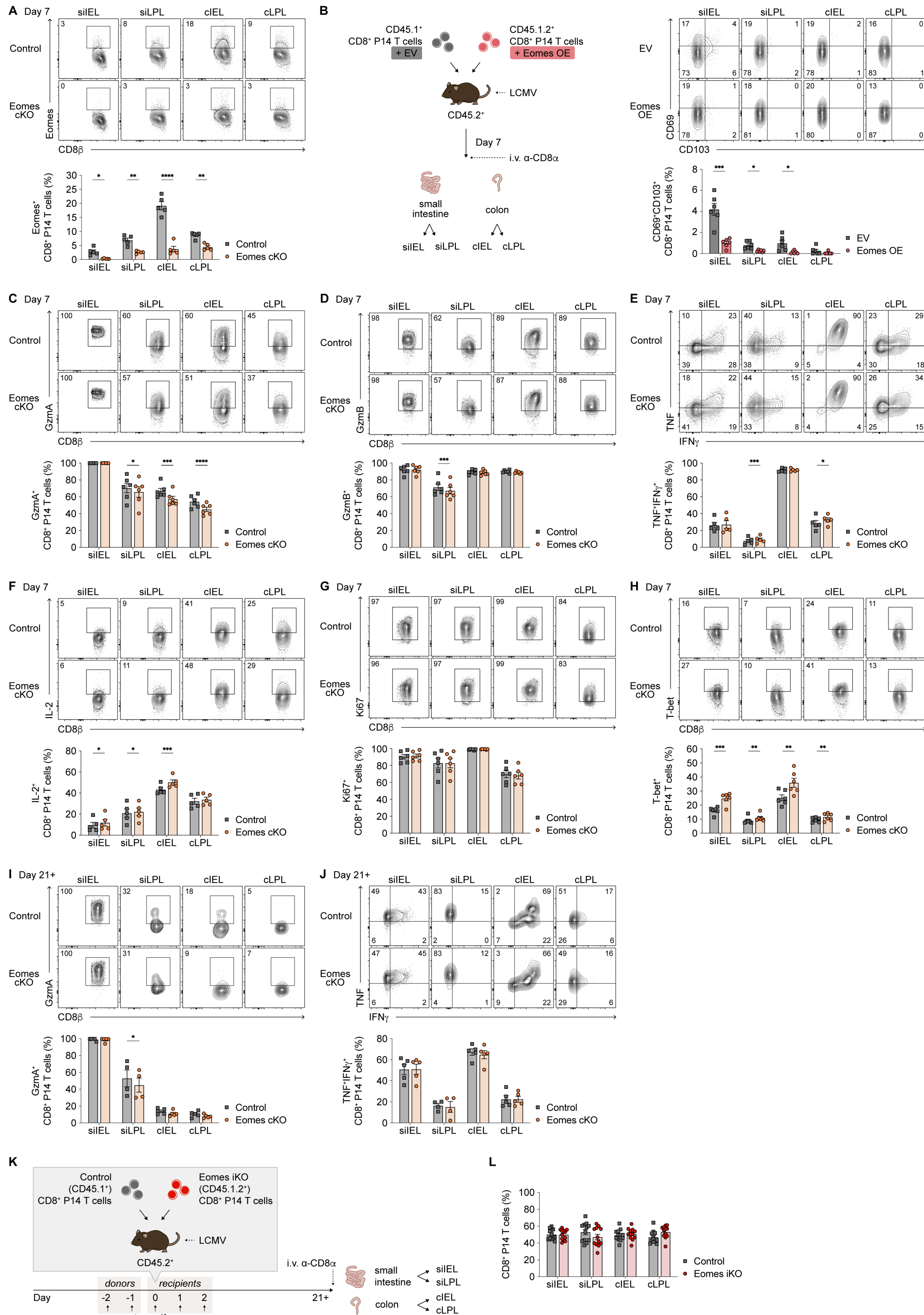

A Day 7
siIEL
siLPL
cIEL
cLPL
Control
Eomes cKO
Eomes
CD8β
Eomes+ CD8+ P14 T cells (%)
Control
Eomes cKO
B
CD45.1+ CD8+ P14 T cells + EV
CD45.1.2+ CD8+ P14 T cells + Eomes OE
LCMV
CD45.2+
Day 7
i.v. α-CD8α
small intestine
colon
EV
Eomes OE
CD69
CD103
CD69+CD103+ CD8+ P14 T cells (%)
C Day 7
GzmA
GzmA+ CD8+ P14 T cells (%)
D Day 7
GzmB
GzmB+ CD8+ P14 T cells (%)
E Day 7
TNF
IFNγ
TNF+IFNγ+ CD8+ P14 T cells (%)
F Day 7
IL-2
IL-2+ CD8+ P14 T cells (%)
G Day 7
Ki67
Ki67+ CD8+ P14 T cells (%)
H Day 7
T-bet
T-bet+ CD8+ P14 T cells (%)
I Day 21+
J Day 21+
K
Control (CD45.1+) CD8+ P14 T cells
Eomes iKO (CD45.1.2+) CD8+ P14 T cells
donors
recipients
Day
tamoxifen
L
CD8+ P14 T cells (%)
Eomes iKO

Figure S6. Deficiency of Eomes has modest effects on intestinal CD8^{+} T cell differentiation, Related to Figure 5.

(A and C–H) CD8^{+} T cells from control (CD45.1^{+}) and *Eomes*$^{fl/fl}$*Cd4-Cre*$^{+}$(CD45.1.2^{+}, Eomes cKO) P14 mice were mixed at a 1:1 ratio and adoptively co-transferred into congenic CD45.2^{+} recipients prior to infection with LCMV; gated i.v.-negative siIEL, siLPL, cIEL, and cLPL CD8^{+} T cells were analyzed at 7 days post-infection. Representative flow cytometry plots (top) and bar graphs displaying frequencies of control (grey squares) vs. Eomes cKO (orange circles) P14 T cells expressing Eomes (**A**), GzmA (**C**), GzmB (**D**), TNF and IFNγ (**E**), IL-2 (**F**), Ki67 (**G**), or T-bet (**H**); numbers represent the frequencies of cells within each gate. For analyses of TNF, IFNγ, and IL-2, cells were restimulated *in vitro* for 3h with gp_{33-41} peptide. **(B)** CD8^{+} T cells from wild-type CD45.1^{+} P14 or wild-type CD45.1.2^{+} P14 mice were activated and transduced with empty vector (EV) or Eomes overexpression (Eomes OE) constructs, respectively. Cells were mixed at a 1:1 ratio and adoptively co-transferred into congenic CD45.2^{+} hosts that were subsequently infected with LCMV; gated i.v.-negative siIEL, siLPL, cIEL, and cLPL CD8^{+} T cells were analyzed at 7 days post-infection. Representative flow cytometry plots (top) displaying CD69 and CD103 expression by EV vs. Eomes OE P14 T cells. Bar graph (bottom) representing frequencies of CD69^{+}CD103^{+} EV vs. Eomes OE P14 T cells. **(I and J)** Representative flow cytometry plots (top) and bar graphs (bottom) displaying GzmA (**I**) and TNF and IFNγ (**J**) expression by control vs. Eomes cKO P14 T cells after 21 days following infection. For analyses of TNF and IFNγ, cells were restimulated *in vitro* for 3h with gp_{33-41} peptide. **(K)** Experimental design. Control (CD45.1^{+}) and *Eomes*$^{fl/fl}$*Ert2-Cre*$^{+}$ (CD45.1.2^{+}, Eomes iKO) P14 donor mice were treated with tamoxifen i.p. for 2 days prior to sacrifice. CD8^{+} T cells from control and Eomes iKO P14 donor mice were mixed at a 1:1 ratio and adoptively co-transferred into congenic CD45.2^{+} recipients 30 minutes

prior to infection with LCMV. Intraperitoneal tamoxifen injections were continued on the day of infection and on days 1 and 2 post-infection; siIEL, siLPL, cIEL, and cLPL compartments were harvested and analyzed after day 21 post-infection.

(L) Quantification of the proportions of control (gray squares) vs. Eomes iKO (red circles) $CD8^+$ P14 cells in each intestinal tissue compartment.

Data are represented as mean ± SEM. Paired *t*-test. *p<0.05, **p<0.01, ***p<0.001 ****p<0.0001. Data are representative of at least 3 independent experiments with n=5-6 mice per experiment.

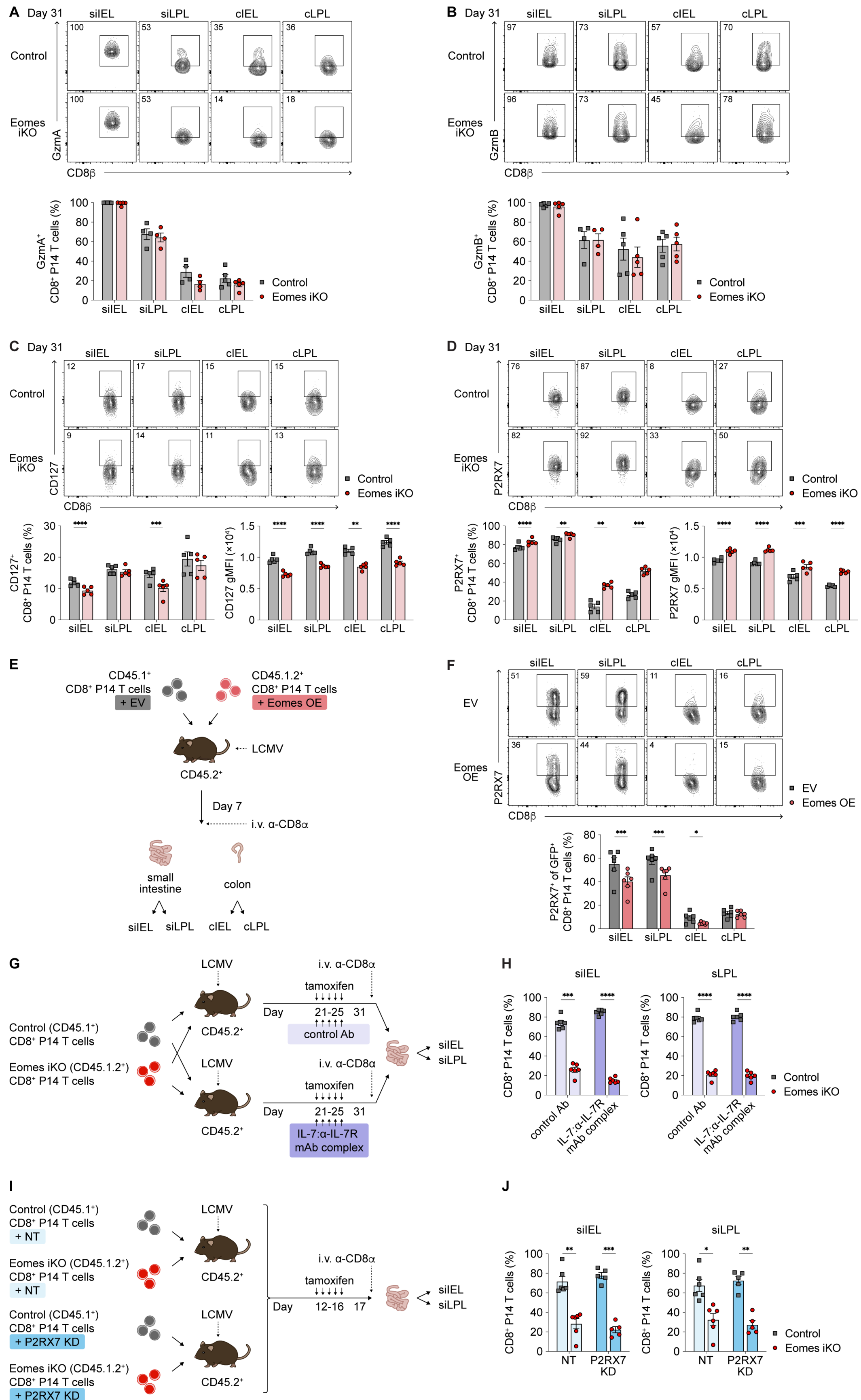

A Day 31
siIEL
siLPL
cIEL
cLPL
Control
Eomes iKO
GzmA
CD8β
GzmA⁺ CD8⁺ P14 T cells (%)
B Day 31
GzmB
GzmB⁺ CD8⁺ P14 T cells (%)
C Day 31
CD127
CD127⁺ CD8⁺ P14 T cells (%)
CD127 gMFI (×10⁴)
D Day 31
P2RX7
P2RX7⁺ CD8⁺ P14 T cells (%)
P2RX7 gMFI (×10⁴)
E
CD45.1⁺ CD8⁺ P14 T cells
+ EV
CD45.1.2⁺ CD8⁺ P14 T cells
+ Eomes OE
LCMV
CD45.2⁺
Day 7
i.v. α-CD8α
small intestine
colon
F
EV
Eomes OE
P2RX7⁺ of GFP⁺ CD8⁺ P14 T cells (%)
G
Control (CD45.1⁺) CD8⁺ P14 T cells
Eomes iKO (CD45.1.2⁺) CD8⁺ P14 T cells
tamoxifen
Day 21-25 31
control Ab
IL-7:α-IL-7R mAb complex
H
sLPL
CD8⁺ P14 T cells (%)
I
+ NT
+ P2RX7 KD
Day 12-16 17
J
NT
P2RX7 KD

Figure S7. Transcriptional analyses identify putative regulators of small intestine CD8$^+$ T$_{RM}$ cell maintenance, Related to Figures 6 and 7.

(A and B) Representative flow cytometry plots (top) displaying GzmA (**A**) and GzmB (**B**) expression by gated i.v.-negative control vs. Eomes iKO P14 T cells in each intestinal tissue compartment at day 31 post-infection; numbers represent the frequencies of cells within each gate. Bar graphs (bottom) indicate the frequencies of control vs. Eomes iKO P14 T cells expressing each molecule. **(C and D)** Representative flow cytometry plots (top) displaying CD127 (**C**) and P2RX7 (**D**) expression by gated i.v.-negative control vs. Eomes iKO P14 T cells in each intestinal tissue compartment. Bar graphs indicate the frequencies of control vs. Eomes iKO P14 T cells expressing each molecule (bottom left) and the expression of each molecule on a per-cell basis (gMFI) (bottom right) at day 31 post-infection. **(E)** Experimental design. CD8$^+$ T cells from wild-type CD45.1$^+$ or wild-type CD45.1.2$^+$ P14 T cells were activated and transduced with empty vector (EV) or Eomes overexpression (Eomes OE) constructs, respectively. Cells were mixed at a 1:1 ratio and adoptively co-transferred into congenic CD45.2$^+$ hosts that were subsequently infected with LCMV. Small intestine IEL, siLPL, cIEL, and cLPL CD8$^+$ T cells were isolated at 7 days post-infection. **(F)** Representative flow cytometry plots (top) displaying P2RX7 expression by gated i.v.-negative EV vs. Eomes OE P14 T cells. Bar graph represents frequencies of cells expressing P2RX7. **(G)** Experimental design. CD8$^+$ T cells from control (CD45.1$^+$) or *Eomes*$^{fl/fl}$*Ert2-Cre*$^+$(CD45.1.2$^+$, Eomes iKO) P14 mice were adoptively co-transferred into congenic CD45.2$^+$ recipients prior to infection with LCMV. Mice received 5 doses of tamoxifen along with control mAb or IL-7-αIL-7R mAb complexes i.p. once daily starting at day 21 post-infection; siIEL and siLPL CD8$^+$ T cells were harvested 10 days later after day 31 post-infection.

(H) Bar graphs representing frequencies of control mAb-treated wild-type vs. control Ab-treated Eomes iKO P14 T cells (left, light purple bars); and frequencies of IL-7-αIL-7R mAb complex-treated wild-type vs. IL-7-αIL-7R mAb complex-treated Eomes iKO P14 T cells (right, dark purple bars) in the siIEL and siLPL tissue compartments. **(I)** Experimental design. $CD8^+$ T cells from control ($CD45.1^+$) or Eomes iKO ($CD45.1.2^+$) P14 mice were activated and transduced with non-targeting shRNA (NT) or shRNA targeting *P2rx7* (P2RX7 KD). Cells were mixed at a 1:1 ratio and adoptively co-transferred into congenic $CD45.2^+$ hosts that were subsequently infected with LCMV. Mice received 5 doses of tamoxifen i.p. once daily starting on day 12 post-infection; siIEL and siLPL $CD8^+$ T cells were harvested on day 17 post-infection. **(J)** Bar graphs representing frequencies of NT-transduced control vs. NT-transduced Eomes iKO P14 T cells (left, light blue bars); and frequencies of P2RX7 KD-transduced control vs. P2RX7 KD-transduced Eomes iKO P14 T cells (right, dark blue bars) in the siIEL and siLPL tissue compartments. Data are represented as mean ± SEM. Paired *t*-test. *$p<0.05$, **$p<0.01$, ***$p<0.001$ ****$p<0.0001$. Data are representative of at least 3 independent experiments with n=5-6 mice per experiment.